

# Materials and processing aspects of CoCrTa/Cr longitudinal recording media. II. Microstructure

Y. Shen<sup>a),b)</sup>, B. Y. Wong<sup>a)</sup>, and D. E. Laughlin<sup>a)</sup>  
*Carnegie Mellon University, Pittsburgh, Pennsylvania 15213*

(Received 12 March 1993; accepted for publication 16 August 1994)

In the CoCrTa/Cr system, it has been postulated that segregation of nonmagnetic constituents to grain boundaries is responsible for the low noise and high coercivity. However, direct experimental evidence is still lacking. In this investigation, we have carried out microstructural studies using transmission electron microscopy (TEM) and atomic resolution transmission electron microscopy (ARTEM) of CoCrTa/Cr films produced under varying processing conditions. We found that the stacking fault density and the degree of crystalline perfection between the faults is most important in increasing the coercivity and improving signal-noise properties as indicated by  $\Delta M$  measurement. High substrate temperatures and high Cr and Ta concentrations promote the occurrence of the stacking faults in the films. In conjunction with ARTEM results, we propose that these faults provide possible sites for elemental segregation which is partially responsible for reducing the magnetic coupling among the unfaulted hcp regions in the CoCrTa films. We also provide microstructural evidence supporting the picture that the high-frequency mechanical texture lines break the intergranular coupling normal to the texture lines resulting in circumferential anisotropy. Grains are crystallographically correlated to form clusters between the texture lines but such correlation is broken up by the texture lines. This gives rise to an effective shape-induced anisotropy. We believe that the cluster size plays a more important role than does the grain size in determining the magnetic properties of CoCrTa/Cr media. © 1994 American Institute of Physics.

## I. INTRODUCTION

It has been generally accepted that a reduction in the intergranular exchange coupling is critical to obtain low noise magnetic thin film recording media.<sup>1,2</sup> In the CoCrPt/Cr media used successfully for 1 Gbit/in.<sup>2</sup> high density recording, Yogi *et al.* used high sputtering Ar pressures to generate physical separation of grains which apparently leads to the reduced intergranular interaction.<sup>3</sup> Isolation of magnetic grains has also been reported by Yamashita and Chen by controlling the nucleation and growth of the underlayer NiP film in the CoNiPt/NiP system.<sup>4</sup> In sputtered CoCrTa/Cr recording media the low noise and high coercivity have been attributed to the segregation of the nonmagnetic constituents to the grain boundaries.<sup>5</sup> However, little convincing direct experimental evidence has been provided.

Using NMR to investigate the local composition around the Co nuclei in the CoCrTa/Cr films, Maeda *et al.* found that the NMR spectra varied systematically with the substrate temperature ( $T_{\text{sub}}$ ).<sup>6</sup> In conjunction with the chrisanthemum-like patterns obtained through chemical etching, they concluded that segregation occurred within the CoCrTa grains as well as at the grain boundaries, as  $T_{\text{sub}}$  increased. It is well known that the grain boundaries are easily attacked by chemical etching. Moreover, stress, chemical inhomogeneity, and precipitates can all give rise to selective etching,<sup>7</sup> which could result in the chrisanthemum-like patterns. Hence, we believe that additional studies are

required to attribute the chrisanthemum-like patterns exclusively to Cr segregation.

Chan *et al.*<sup>8</sup> investigated the Cr segregation at grain boundaries in heat treated bulk CoCr alloys by energy dispersive x-ray analysis (EDX). No evidence of Cr enrichment at grain boundaries was found within the instrumental resolution (200–500 Å). In the CoCrTa system, Cheong, Feng, and Laughlin<sup>9</sup> have observed Ta rich precipitates ( $\text{Co}_3\text{Ta}$ ,  $\text{L1}_2$ ) in the fcc CoCrTa matrix of  $\text{Co}_{82.8}\text{Cr}_{14.6}\text{Ta}_{2.6}$  target materials, after heat-treatment at 500 °C. It is therefore of interest to find out whether similar types of precipitates or perhaps other forms of segregation can exist in CoCrTa films using atomic resolution transmission electron microscopy (ARTEM) which is a powerful tool to study fine-scale precipitates, as well as the fine structure both in Co grains and at grain boundaries.

Duan *et al.*<sup>10</sup> have attempted to correlate the microstructure with magnetic properties using transmission electron microscopy (TEM) in the CoCrTa/Cr systems. In their studies, the films varied in both crystallographic texture and magnetic properties. Since different crystallographic textures will produce different imaging conditions during observation of the samples by TEM, it is difficult to judge whether the reported change in contrast comes from the change in crystallographic texture or from other effects.

In most commercial Co/Cr media, the substrate disks have been circumferentially textured. This mechanical texture can induce a circumferential magnetic anisotropy and enhance  $H_c$ ,  $S$ , and  $S^*$ .<sup>11,12</sup> As a result, both  $H_c$  and  $M_r$

<sup>a)</sup>Department of Materials Science and Engineering.

<sup>b)</sup>Read-Rite Corporation, 44100 Osgood Rd., Fremont, CA 94539.

measured in the circumferential direction are greater than in the radial direction. The anisotropy has been found to depend on  $T_{\text{sub}}$ , bias voltage, the thickness of the Cr underlayer ( $t_{\text{Cr}}$ ), the thickness of the Co alloy film ( $t_{\text{Co}}$ ), as well as the surface roughness.<sup>11-14</sup> A number of mechanisms have been proposed to explain the origin of this anisotropy. For example, circumferential alignment of the  $c$  axes<sup>11</sup> or acicular grain growth<sup>12</sup> along the circumferential direction have been proposed. More recently, Coughlin *et al.* have suggested that the high-frequency texture lines break the intergranular coupling normal to the texture lines resulting in the circumferential anisotropy.<sup>14</sup> However, no supporting microstructural evidence was provided.

In this study, we first describe a modified routine to the conventional jet-polishing technique developed to prepare plane-view thin film TEM specimens from CoCrTa/Cr recording disks. Then, we present and discuss the microstructure of CoCrTa/Cr films with varying magnetic properties but all having the  $\{11\bar{2}0\}$  crystallographic texture. The defect structure and the possible segregation will be examined using ARTEM. Finally, we will present a picture of the microstructural origin of the magnetic anisotropy which is induced by the mechanical texture.

## II. EXPERIMENTAL PROCEDURES

The ion-milling technique has been widely used to prepare thin film specimens from magnetic recording disks for transmission electron microscopic (TEM) studies. This technique could introduce artifacts caused by the high energy ions. Also it takes a long time to prepare specimens. Furthermore, it is difficult to obtain a large region that is thin enough for observation by the Lorentz technique. Jet electro-polishing is a commonly used technique in metallurgy. The usual apparatus is made up of a specimen holder and a polishing unit with an automatic shut off.<sup>15</sup> Co/Cr thin film magnetic recording disks have a complex composite structure, which consists of five layers of different materials, namely, the Al alloy disk, the amorphous NiP electroless-plated on the disk, the Co/Cr bilayer films, and the protective overcoating. This composite structure has posed difficulties in finding an electrolyte suitable for all these layers. Also, unlike preparing TEM specimens from bulk materials in which both sides of the specimen undergo polishing simultaneously, the film side must remain untouched by the chemical solution. Therefore, it is necessary to find a coating which protects the film surface from the polishing solution, yet is transparent to light so that the polishing process can be automatically stopped as soon as the perforation occurs.

The electrolyte used for CoCrTa magnetic disks in our study contains 15% butyl alcohol (butanol), 65% ethanol, and 20% perchloric acid. The composition is close to that used in jet-polishing CoCr alloys.<sup>16</sup> This solution can polish all the layers in the CoCrTa magnetic disks.

Coupons with area  $1\text{ cm} \times 2\text{ cm}$  were first cut from the disks and the original overcoating of the disks were removed by plasma etching. They were then mechanically polished from the Al side until a thin foil with a thickness of 150 nm was obtained. A number of microstop coatings were tested which would protect the film surface from the polishing so-

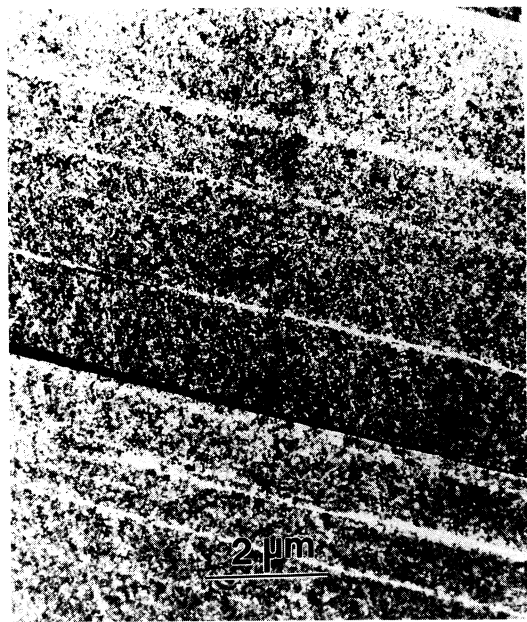


FIG. 1. A bright field image of the CoCrTa magnetic disks using jet-polishing. The stripes shown in the photograph are mechanical texturing lines. The original overcoating on the disk was removed by plasma etching after jet-polishing.

lution, yet would be transparent to light. A solution consisting of a mixture of saturated microstop and acetone with a ratio of 2.5:1 was found to work best. A thin layer of this solution was painted on the film side of the foil and a 3-mm-diam disk was punched from the thin foil after the paint dried. Even though the thin layer of this paint on the film can resist the attack from chemical etching it can not withstand the stream of the electrolyte during jet-polishing. A thin piece of glass (7059 Corning glass) was therefore put over the film side of the 3 mm disk before the cover was screwed into the jet-polishing holder. The polishing started with 30 V and 40 mA with finishing condition 20 V and 25 mA at a temperature ranging from  $0\text{ }^{\circ}\text{C}$  to  $-5\text{ }^{\circ}\text{C}$ . The microstop protective layer was removed by dissolving it in acetone before the sample was examined with a Philips (420T) transmission electron microscope (TEM) and a JEOL 4000EX atomic resolution transmission electron microscope (ARTEM). With this modified routine, we can obtain a large thin area exceeding  $10\text{ }\mu\text{m} \times 10\text{ }\mu\text{m}$ , as shown in Fig. 1 which is much larger than the recording bit size.

## III. RESULTS AND DISCUSSION

### A. Stacking faults

Fringe contrast within the grains has often been observed in Co based longitudinal recording media. Hono *et al.*<sup>17</sup> demonstrated unambiguously that the fringe contrast is due to (0002) stacking faults, which appear to be the dominant structural defect in Co based alloy films. In the CoCr system, Cr additions were found to increase the fault density.<sup>8</sup> The faults and grain boundaries in CoCr bulk alloys have been reported to act as pinning sites which impede domain wall motion.<sup>8</sup> The significance of the faults was pointed out by

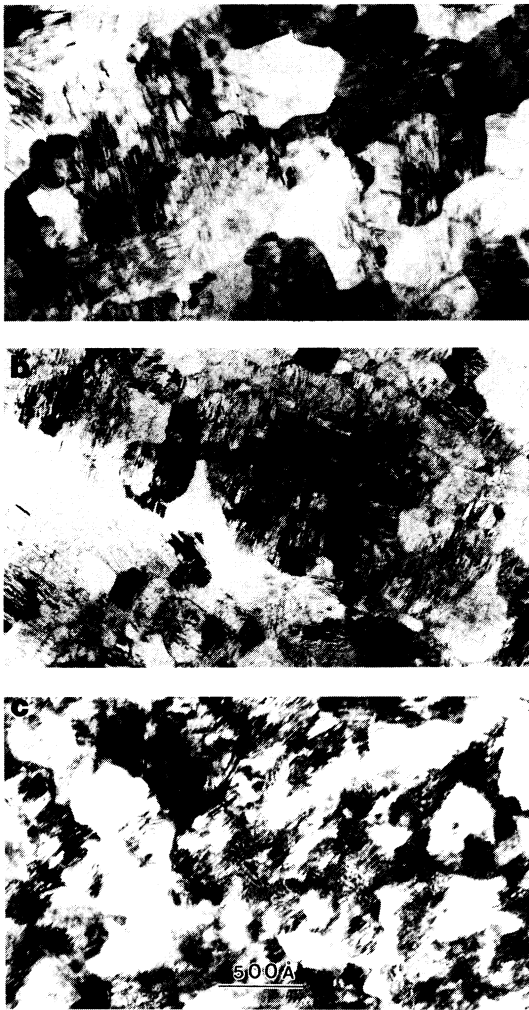


FIG. 2. Bright field TEM images of  $\text{Co}_{82.8}\text{Cr}_{14.6}\text{Ta}_{2.6}(400 \text{ \AA})/\text{Cr}$  films deposited on mechanically textured NiP/Al disks under the conditions (a) Cr: 600 Å, 260 °C; Co: 260 °C; (b) Cr: 150 Å, 260 °C; Co: 260 °C; and (c) Cr: 600 Å, 260 °C; Co: room temperature. The coercivity of these films are 1750, 1622, and 788 Oe, respectively. All films displayed the  $\{11\bar{2}0\}$  texture.

Tang *et al.* in a paper discussing CoNiCr and CoFeCr thin film media.<sup>18</sup> Unfortunately, their conclusions were based on a comparison between two films from different media, i.e., CoNiCr and CoFeCr, both of which have a relatively low  $H_c$  ( $<1000$  Oe). Therefore, it is important to study the effect of the stacking faults on the magnetic properties in the same media and which also have the same crystallographic texture (the  $c$  axis in-plane).

Earlier, we demonstrated that CoCrTa/Cr films, despite having the same  $\{11\bar{2}0\}$  crystallographic texture, could be produced to have drastically different magnetic characteristics when the deposition temperature of the magnetic layer was varied. The bright field TEM images of two such films are displayed in Fig. 2(a) (sample D, where the CoCrTa was deposited at 260 °C) and 2(c) (sample A, where the CoCrTa was deposited at RT). The  $\text{Co}_{82.8}\text{Cr}_{14.6}\text{Ta}_{2.6}$  film, deposited at 260 °C [Fig. 2(a)], has a much higher  $H_c$ , and had a higher stacking fault density. Also the grain boundaries were quite distinct. The regions between faults had a more uniform con-

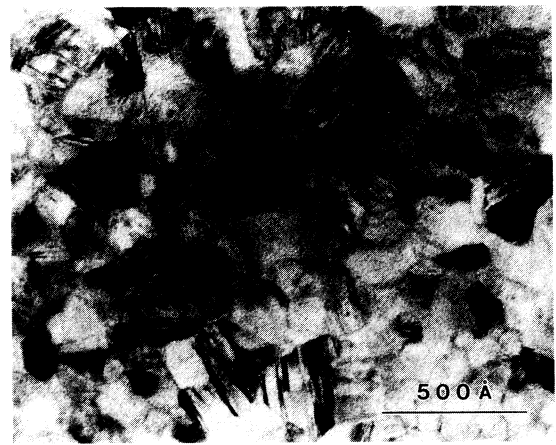


FIG. 3. Bright field image of  $\text{Co}_{86}\text{Cr}_{12}\text{Ta}_2(400 \text{ \AA})/\text{Cr}(600 \text{ \AA})$  film on a mechanically textured NiP/Al disk. The  $H_c$  of the film is 1310 Oe.

trast than those shown in Fig. 2(c), indicating that the elastic strain in those regions was lower.

The impact of a high density of stacking faults can be considered in two ways. First, these faults could provide sites for solute segregation which could reduce exchange coupling between the hcp regions separated by the stacking faults. Elemental segregation at stacking faults has been commonly known as the Suzuki effect.<sup>19</sup> Additionally, the elastic strain in the films would be minimized due to the formation of the high density of stacking faults. If the strain had built up, the magnetocrystalline anisotropy may have decreased thereby lowering the  $H_c$  and noise properties of the films.

In part I of our study (previous article of this issue), we showed that the composition difference in the CoCrTa targets gave different  $H_c$  dependences on Cr bias voltage on pre-heated substrate temperature. The lower Co concentration films ( $\text{Co}_{82.8}\text{Cr}_{14.6}\text{Ta}_{2.6}/\text{Cr}$ ) had much higher  $H_c$  than the Co richer films for a given  $T_{\text{sub}}$ , even though they had a lower  $M_s$ . Fewer stacking faults were observed in the Co rich films ( $\text{Co}_{86}\text{Cr}_{12}\text{Ta}_2/\text{Cr}$ ) as shown in Fig. 3. This also suggests that the higher  $H_c$  of the film with less Co is probably due to a higher density of the faults and therefore possibly more segregation for a given  $T_{\text{sub}}$ .

## B. Grain size

Figure 4 shows the grain size change for two Cr films with different Cr film thickness. As the thickness of the Cr films increases,<sup>3</sup> the grain size also increases. In order to investigate the grain size effect on  $H_c$ , we varied the Cr underlayer thickness at 260 °C while keeping the CoCrTa thickness constant. We found that the increase in  $H_c$  at 260 °C was less than 10% when  $t_{\text{Cr}}$  was increased from 150 to 3000 Å.<sup>20</sup> This indicates that  $H_c$  of the CoCrTa films is not strongly influenced by the Cr underlayer grain size.

Figure 2(b) displays the TEM bright field image of a  $\text{Co}_{82.8}\text{Cr}_{14.6}\text{Ta}_{2.6}(400 \text{ \AA})/\text{Cr}(150 \text{ \AA})$  film deposited at 260 °C. The  $H_c$  of this film is quite similar to that of the film formed on 600 Å Cr [Fig. 2(a)]. This also shows that the underlayer

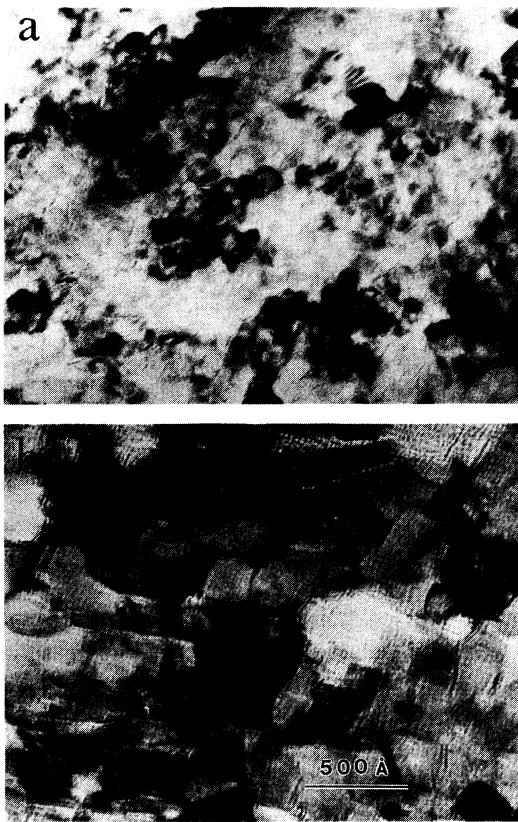


FIG. 4. The microstructure of Cr films deposited on NiP/Al disks at room temperature with thickness of (a) 360 Å and (b) 1470 Å.

grain size does not strongly effect the  $H_c$  of the CoCrTa films.

It is worth pointing out that the grain size of the Co film is often not well defined. When the magnetic layer is deposited at room temperature, the grain boundaries are not distinct. On the other hand, when the magnetic layer is deposited at 260 °C with the underlayer of Cr having the {200} crystallographic texture, two crystallographic variants of the CoCrTa grains can form on each of the Cr grains, with their  $c$  axes normal to each other.<sup>21</sup> Additionally, the CoCrTa grains have low angle grain boundaries and form clusters with closely related crystallographic orientation. The size of these clusters plays an important role in determining the magnetic properties of the films because magnetic coupling among the grains in the cluster should be strong. More results on cluster formation will be discussed in Sec. III D.

### C. ARTEM and segregation

To maximize the grain growth and segregation, a mechanically textured NiP/Al substrate was heated at 260 °C and  $\text{Co}_{82.8}\text{Cr}_{14.6}\text{Ta}_{2.6}$  film was fabricated with a low Cr and CoCrTa sputtering rate of 20 Å/min. Also, a thicker CoCrTa film (800 Å) was sputtered so that it would be easier to remove the Cr underlayer (2500 Å).

The films had a predominant  $\{11\bar{2}0\}_{\text{Co}}/\{200\}_{\text{Cr}}$  crystallographic texture, revealed by selected area diffraction. Figure 5 displays the ARTEM image of one of the CoCrTa grains

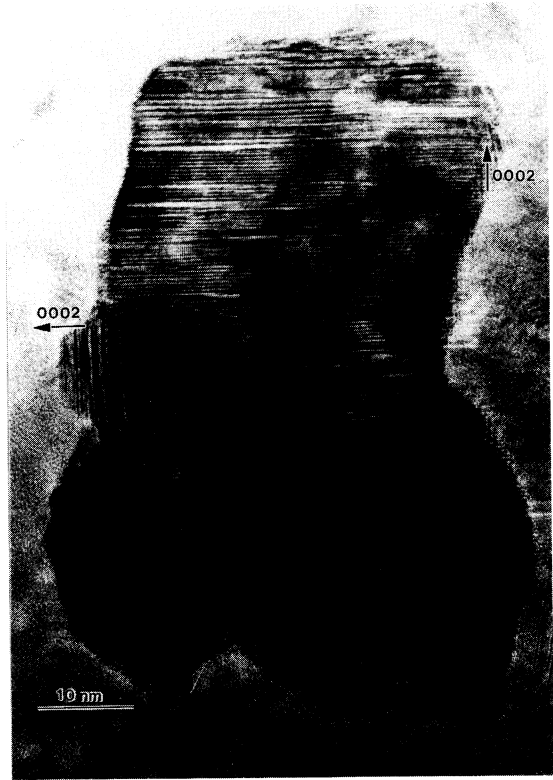


FIG. 5. An overall ARTEM image of one CoCrTa grain, with a  $\{11\bar{2}0\}$  plane in the plane of a  $\text{Co}_{82.8}\text{Cr}_{14.6}\text{Ta}_{2.6}$  film with a Cr underlayer thickness of 2500 Å deposited at 260 °C.

with a  $(11\bar{2}0)$  orientation. The most striking feature of the image is the existence of the high density of faults. Two crystallographic variants with their  $c$  axes normal to each other are present. The origin of the two variants has been discussed by Wong *et al.*<sup>21,22</sup>

Unlike the bulk  $\text{Co}_{82.8}\text{Cr}_{14.6}\text{Ta}_{2.6}$  target materials where ordered  $\text{Co}_3\text{Ta}$  precipitates grew from the fcc matrix after the heat treatment,<sup>9</sup> no precipitates have been observed either inside the hcp CoCrTa grains or at their grain boundaries. Since the segregation could occur near the stacking faults,<sup>19</sup> EDS is not an effective technique to investigate the Suzuki effect because of its spatial limitation. However, such solute enhancement near stacking faults has been directly observed in other Co alloys (Co-0.98 at. % Nb and Co-0.98 at. % Fe) by the atom-probe field-ion microscope.<sup>23,24</sup> Since the CoCrTa films produced at elevated substrate temperatures had more faults, we propose that it is segregation to the stacking faults which causes the increase in  $H_c$ . Such segregation would reduce the intergranular exchange coupling between unfaulted hcp regions in the CoCrTa/Cr system, thereby increasing  $H_c$  and perhaps also reducing the noise.

### D. Mechanical texture

We performed microstructural studies on the  $\text{Co}_{82.8}\text{Cr}_{14.6}\text{Ta}_{2.6}$  (400 Å)/Cr(600 Å) films sputtered on textured NiP/Al at both RT and 260 °C. The ratios of  $H_{c\parallel}/H_{c\perp}$  and  $m_{r\parallel}/m_{r\perp}$  ranged from 1.1 to 1.5 and 1.1 to 1.3, respectively. Figure 6 shows a pair of bright and dark field images

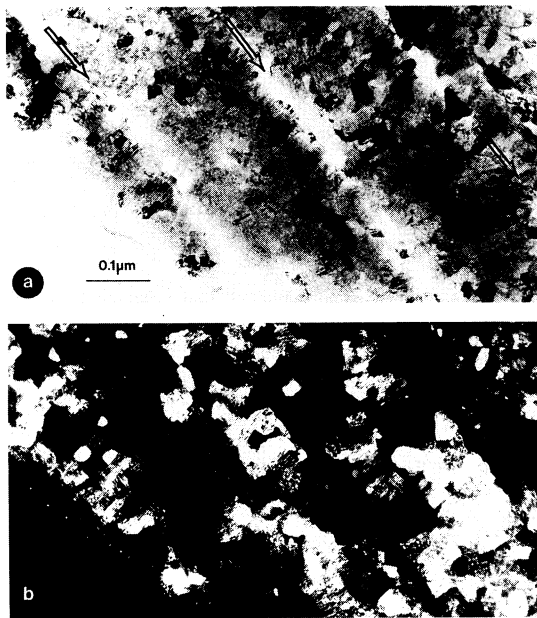


FIG. 6. A pair of bright and dark field images of a  $\text{Co}_{82.8}\text{Cr}_{14.6}\text{Ta}_{2.6}(400 \text{ \AA})/\text{Cr}(150 \text{ \AA})$  film prepared at  $260 \text{ }^\circ\text{C}$ .

of a  $\text{Co}_{82.8}\text{Cr}_{14.6}\text{Ta}_{2.6}(400 \text{ \AA})$  film with Cr underlayer thickness of  $150 \text{ \AA}$ . The  $H_c$ ,  $S$ , and  $S^*$  of the film in the circumferential and radial directions are listed in Table I. The dark field image reveals that grains grown between two adjacent texture lines were grouped as clusters which are crystallographically correlated. We believe that the intergranular magnetic coupling within these clusters would be strong. Such correlation is, however, broken up by the texture lines. This would give rise to an effective shape-induced anisotropy. This finding supports the picture that the high-frequency texture lines break the intergranular coupling normal to the texture lines, resulting in the circumferential anisotropy.<sup>14</sup>

Figure 7 shows a magnified image of a cluster of grains consisting of two crystallographic variants of CoCrTa as well as low angle grain boundaries. Since the Cr underlayer is only  $150 \text{ \AA}$  thick, this cluster could not be grown on only one Cr grain. Thus, neighboring Cr grains at high sputtering temperatures also appear to grow on their substrate with closely related crystallographic orientation. It can be seen that such a correlation is stopped at the mechanical texture line.

The micrographs displayed in Figs. 6 and 7 show that CoCrTa grains were more or less equiaxed in shape. Also, the intensity of all the selected area diffraction (SAD) patterns did not show significant variation around the rings over regions of the order of the SAD aperture (Fig. 8). This indi-

TABLE I. The  $H_c$ ,  $S$ , and  $S^*$  in circumferential direction and radial direction are listed for the  $\text{Co}_{82.8}\text{Cr}_{14.6}\text{Ta}_{2.6}(400 \text{ \AA})/\text{Cr}(150 \text{ \AA})$  film deposited on circumferentially textured NiP/Al disk at  $260 \text{ }^\circ\text{C}$ .

	$H_c$ (Oe)	$S$	$S^*$
Circumferential direction	1622	0.93	0.91
Radial direction	1322	0.78	0.67

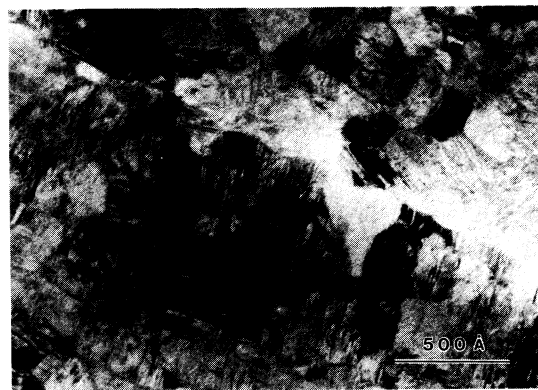


FIG. 7. A magnified region containing a cluster of grains near the mechanical texture line.

cates that the Co and Cr films did not possess in-plane crystallographic texture in spite of the forming clusters between the texture lines. These results indicate that the circumferential anisotropy does not originate from the alignment of the  $c$  axes or acicular grains along the texture lines (compare Refs. 11–13).

#### IV. CONCLUSIONS

We have performed studies on the relationship among processing, microstructure, and magnetic properties of CoCrTa/Cr longitudinal recording media. Our findings are as follows:

- (1) A high density of the stacking faults and the degree of crystal perfection between the faults are most critical for obtaining high  $H_c$  and low noise CoCrTa/Cr recording media as indicated by  $\Delta M$  measurement. High substrate temperature and high Cr and Ta concentration promote the formation of stacking faults.
- (2) No precipitation of a secondary phase was observed either at grain boundaries or inside CoCrTa grains using ARTEM. We believe that the stacking faults, and possi-

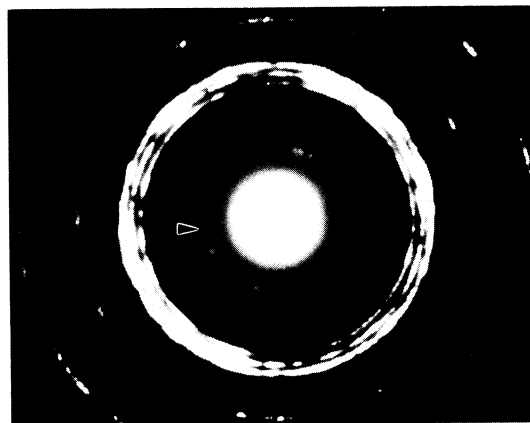


FIG. 8. SAD pattern of the film shown in Figs. 8 and 9 using a  $1 \text{ mm}$  aperture. The presence of the (0001) ring indicated by the arrow is due to double diffraction and shows that the film is strongly textured with the  $c$  axes in the plane of the film.

- bly the grain boundaries, provide sites for elemental segregation. Elemental segregation to the stacking faults (the Suzuki effect) could be responsible for reducing the exchange intergranular interaction, and consequently, gives rise to the higher  $H_c$  and better noise properties.
- (3) The enhancement in  $H_c$  at elevated  $T_{\text{sub}}$  is not strongly influenced by the Cr underlayer grain size. The grain size of the CoCrTa films is ill-defined because of the formation of clusters of grains in the films prepared with high  $T_{\text{sub}}$  and lack of distinctive grain boundaries for the film deposited at low temperature. The size of these clusters will influence the magnetic properties of the films.
  - (4) We have developed a modified routine of conventional jet-polishing technique used to prepare thin film TEM specimens from CoCrTa/Cr magnetic disks. The preparation of TEM specimens with this technique takes considerably less time than the ion-milling technique, and eliminates possible artifacts induced by ion-beam.
  - (5) We also have provided the microstructural evidence supporting the picture that the high-frequency texture lines break the intergranular coupling normal to the texture lines resulting in the circumferential anisotropy. Grains are crystallographically correlated to form clusters between the texture lines but such correlation is broken up by the texture lines. This give rise to an *effective shape-induced* anisotropy.

#### ACKNOWLEDGMENTS

The financial support of Hitachi Metals, Inc. for this research is gratefully acknowledged. The facilities used for this research are in part supported by NSF under grant No. ECD-8907068.

- <sup>1</sup>J. G. Zhu and H. N. Bertram, *J. Appl. Phys.* **63**, 3248 (1988).
- <sup>2</sup>T. Chen and T. Yamashita, *IEEE Trans. Magn.* **MAG-24**, 2700 (1988).
- <sup>3</sup>T. Yogi, C. Tsang, T. A. Nguyen, K. Ju, G. L. Gorman, and G. Castillo, *IEEE Trans. Magn.* **MAG-26**, 2271 (1990).
- <sup>4</sup>T. Yamashita and T. Chen, *IEEE Trans. Magn.* **MAG-27**, 4127 (1991).
- <sup>5</sup>J. A. Christner, R. Ranjan, R. L. Peterson, and J. I. Lee, *J. Appl. Phys.* **63**, 3260 (1988).
- <sup>6</sup>Y. Maeda and K. Takei, *IEEE Trans. Magn.* **MAG-27**, 4121 (1991).
- <sup>7</sup>U. R. Evans, *An Introduction to Metallic Corrosion* (Arnold, London, 1948), pp. 114–122.
- <sup>8</sup>L. H. Chan, G. Thomas, and J. S. Gau, *J. Magn. Magn. Mater.* **79**, 95 (1989).
- <sup>9</sup>B. Cheong, Y. C. Feng, and D. E. Laughlin, *Scripta Metall. Mater.* **30**, 1419 (1994).
- <sup>10</sup>S. Duan, M. R. Khan, J. E. Haeefele, L. Tang, and G. Thomas, *IEEE Trans. Magn.* **MAG-28**, 3258 (1992).
- <sup>11</sup>E. Teng and N. Ballard, *IEEE Trans. Magn.* **MAG-22**, 579 (1986).
- <sup>12</sup>E. M. Simpson, P. B. Narayan, G. T. K. Swami, and J. L. Chao, *IEEE Trans. Magn.* **MAG-23**, 3405 (1987).
- <sup>13</sup>T. Lin, R. Alani, and D. N. Lambeth, *J. Magn. Magn. Mater.* **78**, 213 (1989).
- <sup>14</sup>T. Coughlin, J. Pressesky, S. Lee, N. Heiman, R. D. Fisher, and K. Merchant, *J. Appl. Phys.* **67**, 4689 (1990).
- <sup>15</sup>R. D. Schoone and E. A. Fischione, *Rev. Sci. Instrum.* **37**, 1371 (1966).
- <sup>16</sup>J. W. Edington, *Practical Electron Microscopy in Materials Science* (Philips Technical Library, Eindhoven, 1975).
- <sup>17</sup>K. Hono, B. G. Demczyk, and D. E. Laughlin, *Appl. Phys. Lett.* **55**, 229 (1989).
- <sup>18</sup>L. Tang, G. Thomas, M. R. Khan, S. L. Duan, and N. Heiman, *J. Appl. Phys.* **69**, 5166 (1991).
- <sup>19</sup>H. Suzuki, *J. Phys. Soc. Jpn.* **17**, 322 (1962).
- <sup>20</sup>Y. Shen, D. N. Lambeth, and D. E. Laughlin, *IEEE Trans. Magn.* **MAG-28**, 3261 (1992).
- <sup>21</sup>B. Y. Wong, D. E. Laughlin, and D. N. Lambeth, *IEEE Trans. Magn.* **MAG-27**, 4733 (1991).
- <sup>22</sup>B. Y. Wong, Y. Shen, and D. E. Laughlin, *J. Appl. Phys.* **73**, 418 (1993).
- <sup>23</sup>R. Herschitz and D. N. Seidman, *Acta Metall.* **33**, 1547 (1985).
- <sup>24</sup>R. Herschitz and D. N. Seidman, *Acta Metall.* **33**, 1565 (1985).